JACS
JOURNAL OF THE AMERICAN CHEMICAL SOCIETY
Communication
pubs.acs.org/JACS

Protonation Equilibrium and Hydrogen Production by a Dinuclear Cobalt–Hydride Complex Reduced by Cobaltocene with Trifluoroacetic Acid

Sukanta Mandal,[†] Shinya Shikano,[‡] Yusuke Yamada,[‡] Yong-Min Lee,[†] Wonwoo Nam,*[,†] Antoni Llobet,*[,†,§] and Shunichi Fukuzumi*[,†,‡]

[†]Department of Bioinspired Science, Department of Chemistry and Nano Science, Ewha Womans University, Seoul 120-750, Korea

[‡]Department of Material and Life Science, Graduate School of Engineering, ALCA, Japan Science and Technology Agency, Osaka University, Suita, Osaka 565-0871, Japan

[§]Institute of Chemical Research of Catalonia (ICIQ), Avinguda Països Catalans 16, E-43007 Tarragona, Spain

Supporting Information

ABSTRACT: A dinuclear Co complex with bis(pyridyl)-pyrazolato (bpp^-) and terpyridine (trpy) ligands, $[Co^{III}_2(trpy)_2(\mu\text{-}bpp)(OH)(OH_2)]^{4+}$ ($\mathbf{1}^{4+}$), undergoes three-electron reduction by cobaltocene in acetonitrile to produce $\mathbf{1}^+$, which is in the protonation equilibrium with the $Co^{II}Co^{III}$–hydride complex, and the further protonation of the hydride by trifluoroacetic acid yields hydrogen quantitatively. The kinetic study together with the detection of the $Co^{II}Co^{III}$-hydride complex revealed the mechanism of the hydrogen production by the reaction of $\mathbf{1}^+$ with trifluoroacetic acid.

The continuous consumption of fossil fuels and consequently the increase of CO_2 levels in the atmosphere have become a major concern to search for carbon-free renewable energy resources to solve increasing global energy demands.[1] Hydrogen-based economy is the most desirable and environmentally benevolent.[2−5] Pt is currently used as an efficient electrocatalyst for the reduction of protons to hydrogen (H_2).[6] However, the scarcity and high cost of Pt have severely limited large-scale applications. Thus, the feasibility of the H_2-based economy depends on the design of efficient catalysts based on earth abundant metals. In this context, Co-based proton-reduction catalysts have gained interest in recent years.[7−9] A mononuclear cobaloxime and related complexes have been shown to act as efficient electrocatalysts for H_2 evolution in protic media at relatively low overpotentials.[10−15] Extensive efforts have been devoted to elucidate the mechanism of H_2 evolution by mononuclear Co complexes.[10−15] The formation of Co^{III}–H via the protonation of Co^I species is proposed to be a key step for H_2 evolution catalyzed by the Co complexes. H_2 can be evolved from Co^{III}–H by three different pathways (Scheme 1).[7] Co^{III}–H either can be protonated and release H_2 in the heterolytic pathway or can be reduced to form Co^{II}–H which can react via a similar heterolytic pathway to generate H_2. Alternatively, two Co^{III}–H complexes can combine bimolecularly and release H_2 by the reductive elimination reaction. Gray et al. suggested the latter reaction pathway is the most energetically favorable.[7] Binuclear Co complexes as proton-reduction catalysts merit special attention, because the homolytic pathway could take place in a unimolecular or bimolecular manner depending on ligand design. Peters et al. developed dicobalt macrocycles based on pyridazine dioxime precursors, which act as electrocatalysts for H_2 evolution from 2,6-dichloroanilinium tetrafluoroborate in acetonitrile.[16] However, the mechanism of the proton reduction with a dinuclear Co catalyst has yet to be clarified. We report herein the detailed kinetics and mechanism of proton reduction of trifluoroacetic acid (CF_3COOH) to H_2 by using a dinuclear Co complex with bis(pyridyl)pyrazolato (bpp^-) and terpyridine (trpy) ligands, $[Co^{III}_2(trpy)_2(\mu\text{-}bpp)(OH)(OH_2)]^{4+}$ ($\mathbf{1}^{4+}$) (Figure 1a), which was reduced step-by-step by decamethylcobaltocene ($Co(Cp^*)_2$) and cobaltocene ($Co(Cp)_2$) in acetonitrile (MeCN).

Scheme 1

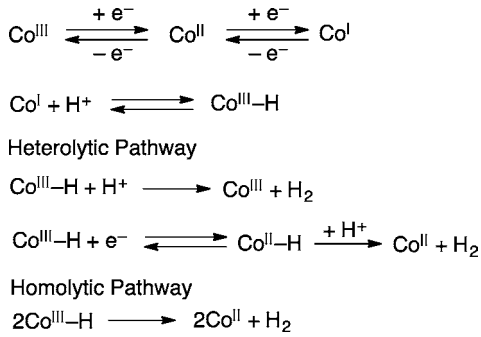

The X-ray crystal structure of $\mathbf{1}^{4+}$ was reported previously, exhibiting that the aqua and hydroxo ligands are coordinated to two Co nuclei sharing a proton.[17] The long distance between two Co centers in $\mathbf{1}^{4+}$ (4.343 Å) may seem to preclude a reductive–elimination reaction, because the two Co–H units are separated too far away for an intramolecular interaction. However, the flexibility of the ligand scaffold may allow interaction between the two hydrides to enable the reductive–elimination reaction. In order to confirm structural flexibility we have synthesized a chloro-bridged dinuclear Co complex, $[Co^{II}_2(trpy)_2(\mu\text{-}bpp)(\mu\text{-}Cl)](PF_6)_2$. The X-ray crystal structure

Received: August 5, 2013
Published: September 25, 2013

   dx.doi.org/10.1021/ja408080z | J. Am. Chem. Soc. 2013, 135, 15294−15297

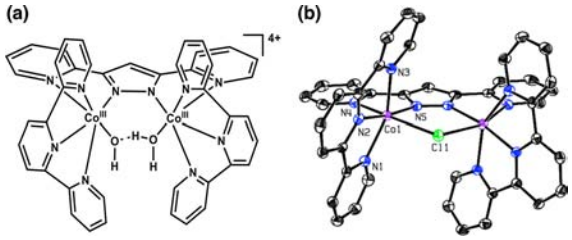

Figure 1. (a) Structure of $[Co^{III}_2(trpy)_2(\mu\text{-bpp})(OH)(OH_2)]^{4+}$ ($\mathbf{1}^{4+}$) and (b) ORTEP plot (50% probability) of the crystal structure of the cationic part of $[Co^{II}_2(trpy)_2(\mu\text{-bpp})(\mu\text{-Cl})](PF_6)_2$ (H atom and counteranions have been omitted for clarity).

of Cl-bridged dimer (Figure 1b and Table S1) reveals that the Co−Co distance (3.953 Å, see Table S2) is shortened by 0.39 Å as compared to that of $\mathbf{1}^{4+}$.

The cyclic voltammogram of $\mathbf{1}^{4+}$ in MeCN shows four Co-centered one-electron reduction waves and two overlapping ligand-centered ones (Figure 2a). The irreversible reduction

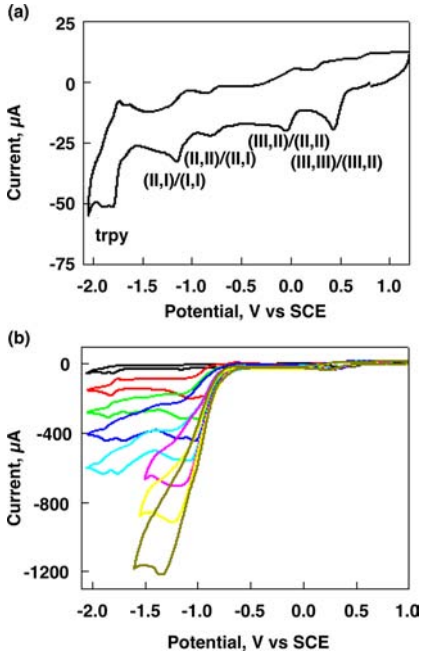

Figure 2. (a) CVs of complex $\mathbf{1}^{4+}$ (1 mM) in 0.1 M n-Bu_4NPF_6 in MeCN and (b) with subsequent additions of CF_3COOH: (from top to bottom) $\mathbf{1}^{4+}$ (1 mM) with no acid, 10, 20, 30, 40, 50, 70, and 100 mM CF_3COOH. Conditions: glassy carbon electrode (inner diameter 3 mm), scan rate = 100 mV s^{-1}.

wave at 0.42 V vs SCE is assigned to $Co^{III}Co^{III}Co^{II}$ ($\mathbf{1}^{4+}/\mathbf{1}^{3+}$) couple and three quasi-reversible reductions ($E_{1/2}$) at −0.02, −0.78, and −1.09 V vs SCE are assigned to $Co^{III}Co^{II}/Co^{II}Co^{II}$ ($\mathbf{1}^{3+}/\mathbf{1}^{2+}$), $Co^{II}Co^{II}/Co^{II}Co^{I}$ ($\mathbf{1}^{2+}/\mathbf{1}^{+}$), and $Co^{II}Co^{I}/Co^{I}Co^{I}$ ($\mathbf{1}^{+}/\mathbf{1}$) couples, respectively, because the reduction currents of these redox couples were comparable to that of ferrocenium/ferrocene in the same concentration as $\mathbf{1}^{4+}$ and no reduction peaks of ligand molecules appeared at the potential higher than −1.7 V vs SCE as indicated in Figure S1b. Addition of the varying amounts of CF_3COOH (E^o = −0.51 V vs SCE and pK_a = 12.0 in MeCN) triggers catalytic currents at potentials near the couple of $\mathbf{1}^{2+}/\mathbf{1}^{+}$ (Figure 2b). Cyclic voltammograms of CF_3COOH in the absence of $\mathbf{1}^{4+}$ exhibit no catalytic current at the potential of the couple of $\mathbf{1}^{2+}/\mathbf{1}^{+}$, suggesting that proton reduction to H_2 occurs with $\mathbf{1}^{+}$ (Figure S1 in SI). H_2 was generated by electrolysis at an applied potential of E = −1.1 V vs SCE for 10 min with a Faradaic yield of 79% based on the the amount of H_2 produced determined by GC (Figure S2 in SI).

The ability of $\mathbf{1}^{n+}$ in different oxidation states (n = 0−2) to reduce protons was examined by the redox titration of $\mathbf{1}^{4+}$ reduced by $Co(Cp)_2$ and $Co(Cp^*)_2$ and the subsequent reaction with protons of CF_3COOH in MeCN. Stepwise reduction of $\mathbf{1}^{4+}$ was performed by using $Co(Cp^*)_2$ as a reductant. The one-electron oxidation potential of $Co(Cp^*)_2$ (E_{ox} = −1.53 V vs SCE) is lower than the one-electron reduction potential of $\mathbf{1}^{+}$. Thus, $\mathbf{1}^{4+}$ undergoes step-by-step reduction to **1**, which exhibits visible and NIR absorption bands at 560 and 1050 nm (black line in Figure 3).

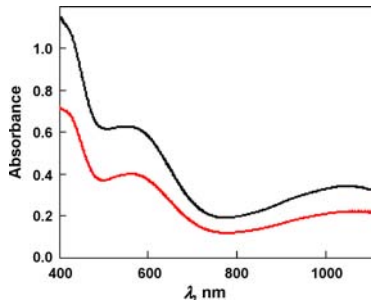

Figure 3. Visible-NIR absorption spectra of the $Co^{II}Co^{I}$ complex ($\mathbf{1}^{+}$: red) and $Co^{I}Co^{I}$ complex (**1**: black) produced by the reduction of $\mathbf{1}^{4+}$ (0.087 mM) with addition of 3 and 4 equiv of $Co(Cp^*)_2$, respectively, in MeCN.

$\mathbf{1}^{+}$ obtained by three-electron reduction of $\mathbf{1}^{4+}$ with 3 equiv of $Co(Cp^*)_2$ also exhibits similar visible and NIR absorption bands at 562 and ∼1100 nm (red line in Figure 3) with approximately half absorbance as compared with **1**. This indicates only little interaction between the two Co moieties. The redox titration of $\mathbf{1}^{4+}$ was also monitored by electron paramagnetic resonance (EPR) spectroscopy. As expected, the starting $\mathbf{1}^{4+}$ and the final **1** were EPR silent. The $\mathbf{1}^{2+}$ was also EPR silent due to the antiferromagnetic interaction between two Co centers at 5.0 K, whereas the $\mathbf{1}^{3+}$ and $\mathbf{1}^{+}$ complexes exhibit EPR spectra due to the paramagnetic Co^{II} species (see Figures S3−S5). $\mathbf{1}^{+}$ was also obtained by the three-electron reduction of $\mathbf{1}^{4+}$ with $Co(Cp)_2$. Because the one-electron oxidation potential of $Co(Cp)_2$ (E_{ox} = −0.9 V vs SCE) is less negative than the E_{red} value of $\mathbf{1}^{+}$, $\mathbf{1}^{+}$ was not further reduced by excess $Co(Cp)_2$.

Addition of excess CF_3COOH to the $\mathbf{1}^{2+}$ obtained by the two-electron reduction of $\mathbf{1}^{4+}$ by 2 equiv of $Co(Cp)_2$ resulted in no production of H_2. However, $\mathbf{1}^{+}$ obtained by the three-electron reduction of $\mathbf{1}^{4+}$ by 3 equiv of $Co(Cp)_2$ reacted with excess CF_3COOH to produce H_2. The amount of H_2 produced was determined by GC (Figures S6−S8).[18] The stoichiometry of the H_2 evolution was determined as given by eq 1.

$$\mathbf{1}^{4+} + 3Co(Cp)_2 + H^+ \rightarrow \mathbf{1}^{2+} + 3Cp(Cp)_2^+ + (1/2)H_2 \quad (1)$$

The time courses of formation of **1** and $\mathbf{1}^{+}$ and the subsequent reactions with protons of CF_3COOH provide valuable information about the mechanism of H_2 evolution. Addition of 4 equiv of $Co(Cp^*)_2$ to a dearated MeCN solution containing $\mathbf{1}^{4+}$ (0.087 mM) resulted in rapid formation of the **1**

dx.doi.org/10.1021/ja408080z | J. Am. Chem. Soc. 2013, 135, 15294−15297

as shown in Figure 4a. Addition of 10 equiv of CF_3COOH to the MeCN solution of **1** resulted in the two-step decay of

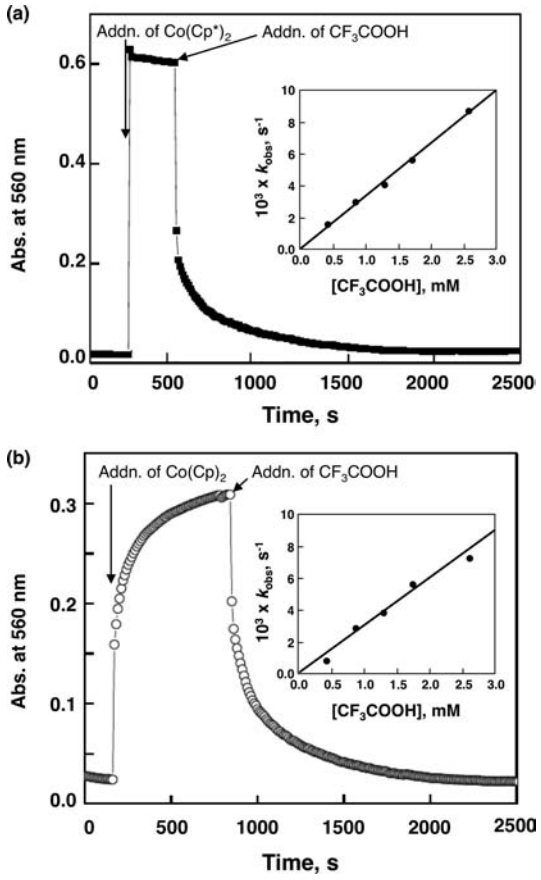

Figure 4. Time profiles of absorbance at 560 nm due to (a) the Co^ICo^I complex (**1**) and (b) the $Co^{II}Co^I$ complex ($\mathbf{1}^+$) with CF_3COOH in dearated MeCN at 298 K. Conditions: [complex] = 0.087 mM and [CF_3COOH] = 0.87 mM. Insets: Plots of k_{obs} vs concentration of CF_3COOH for the second-step reaction of (a) **1** and (b) $\mathbf{1}^+$ with CF_3COOH.

absorbance at 560 nm due to **1** (Figure 4a). In the case of the reaction of $\mathbf{1}^{4+}$ with $Co(Cp)_2$ as shown in Figure 4b, the formation of $\mathbf{1}^+$ was much slower as compared with the reaction of $\mathbf{1}^{4+}$ with $Co(Cp^*)_2$ because of the much more positive oxidation potential of $Co(Cp)_2$ than $Co(Cp^*)_2$ (vide supra). The reaction of the $\mathbf{1}^+$ with CF_3COOH also exhibited two-step decay, i.e., the rapid decay followed by the much slower decay (Figure 4b). The final spectrum corresponds to that due to $\mathbf{1}^{2+}$ as indicated by the stoichiometry (eq 1). The formation of $\mathbf{1}^{2+}$ after the reaction was also confirmed by the EPR spectrum (Figures S3–S5).[19]

The absorbance change in the first rapid step increased with increasing concentration of CF_3COOH for both $\mathbf{1}^+$ and **1** (Figures S9 and S10). The rate of the second slow step obeyed first-order kinetics (see first-order plots in Figures S11 and S12). The observed first-order rate constant (k_{obs}) increased linearly with increasing concentration of CF_3COOH for both $\mathbf{1}^+$ and **1** (Figure 4, insets).

The two-step reaction of **1** with CF_3COOH suggests that the protonation equilibrium of **1** and a hydride complex, $[(Co^{III}–H)(Co^{III}–H)]^{2+}$, occurs first, and then the hydride complex reacts with protons to produce H_2. The first-order dependence of k_{obs} with respect to the concentration of CF_3COOH rules out the homolytic pathway in which H_2 is evolved from the two Co(III)–H moieties to yield $\mathbf{1}^{2+}$. In addition, the similar kinetic behavior in the reaction of $\mathbf{1}^+$ to that in the reaction of **1** (Figure 4, insets) indicates that only one Co^I moiety is enough to produce H_2.

Based on the two-step kinetics, the overall reaction mechanism of H_2 production from the reaction of $\mathbf{1}^+$ is proposed as shown in Scheme 2 (eqs 2–5). First three-electron

Scheme 2

$$[Co^{III}Co^{III}]^{4+} + 3Co(Cp)_2 \rightarrow [Co^{II}Co^{I}]^{+} + 3Co(Cp)_2^{+} \quad (2)$$

$$[Co^{II}Co^{I}]^{+} + H^{+} \rightleftharpoons [Co^{II}Co^{III}–H]^{2+} \quad (3)$$

$$[Co^{II}Co^{III}–H]^{2+} + H^{+} \rightarrow [Co^{II}Co^{III}]^{3+} + H_2 \quad (4)$$

$$[Co^{II}Co^{I}]^{+} + [Co^{II}Co^{III}]^{3+} \rightarrow 2[Co^{II}Co^{II}]^{2+} \quad (5)$$

reduction of the $\mathbf{1}^{4+}$ occurs by 3 equiv $Co(Cp)_2$ to produce the $\mathbf{1}^+$ (eq 2). $\mathbf{1}^+$ is protonated by CF_3COOH to produce the hydride complex ($[Co^{II}Co^{III}–H]^{2+}$), which is in the equilibrium with $\mathbf{1}^+$ (eq 3). The formation of hydride complex during the H_2 evolution was confirmed by the ^1H NMR spectra which exhibits a typical Co(III)–H peak at $\delta = -8.64$ ppm (Figure S13 in SI). The hydride complex reacts with protons to produce H_2 and the $\mathbf{1}^{3+}$ complex (eq 4). This is the rate-determining (the slowest) step for the H_2 production. $\mathbf{1}^{3+}$ is reduced by the $\mathbf{1}^+$ to produce 2 equiv $\mathbf{1}^{2+}$ (eq 5). By summing up eqs 2–5 (2 × eq 2 + eqs 3–5), the overall stoichiometry is the same as the observed one in eq 1.

According to Scheme 2, where the rate-determining step is the reaction of $[Co^{II}Co^{III}–H]^{2+}$, which is formed in the protonation equilibrium of $\mathbf{1}^+$ (eq 3), with CF_3COOH, the rate of decay of $\mathbf{1}^+$ is given by eq 6, where k is the rate constant of

$$-d[(Co^{II}Co^{I})^{+}]/dt = k[H^{+}][(Co^{II}Co^{I})^{+}]/(1 + K[H^{+}]) \quad (6)$$

protonation of the hydride complex to produce H_2 (eq 4) and K is the protonation equilibrium constant of $\mathbf{1}^+$ to produce the hydride complex, $[Co^{II}Co^{III}–H]^{2+}$ (eq 3). Based on the kinetic results (Figure 4b inset and Figure S14), the k and K values at 298 K were determined to be 2.9 M^{-1} s^{-1} and 5.3 × 10^2 M^{-1}, respectively.

In the case of the **1** produced by four-electron reduction of $\mathbf{1}^{4+}$ by 4 equiv $Co(Cp^*)_2$, the k and K values at 298 K were also determined to be 3.3 M^{-1} s^{-1} and 1.1 × 10^3 M^{-1}, respectively (Figure 4a inset and Figure S15). The similar k and K values between the $\mathbf{1}^+$ and **1** indicate that the two Co centers are rather independent, although k and K values of **1** are slightly larger than those of $\mathbf{1}^+$ due to the lower redox potential of the **1** than that of $\mathbf{1}^+$ (Figure 2a).

In conclusion, the $Co^{II}Co^I$ complex ($\mathbf{1}^+$) as well as the Co^ICo^I complex (**1**) produced by the three- and four-electron reduction of a dinuclear Co complex ($\mathbf{1}^{4+}$) with $Co(Cp)_2$ and $Co(Cp^*)_2$, respectively, is protonated by CF_3COOH to produce the hydride complex, which undergoes heterolytic cleavage of the Co(III)–H bond by protons to produce H_2. The preference of the heterolytic cleavage as compared to the homolytic cleavage results from the low redox potentials of $\mathbf{1}^+$ and **1** and the resulting strong basicity of the hydride complexes as suggested by Gray et al.[7]

dx.doi.org/10.1021/ja408080z | J. Am. Chem. Soc. 2013, 135, 15294–15297

■ ASSOCIATED CONTENT

Supporting Information

Experimental section, Tables S1−S3, and Figures S1−S15. This material is available free of charge via the Internet at http://pubs.acs.org.

■ AUTHOR INFORMATION

Corresponding Authors

fukuzumi@chem.eng.osaka-u.ac.jp
wwnam@ewha.ac.kr
allobet@iciq.es

Notes

The authors declare no competing financial interest.

■ ACKNOWLEDGMENTS

This work was supported in part by Grant-in-Aid (nos. 24350069 and 25600025 to Y.Y.) from the MEXT, Japan and by NRF/MEST of Korea through the CRI (2-2012-1794-001-1 to W.N.), GRL (2010-00353 to W.N.) and WCU (R31-2008-000-10010-0 to W.N., S.F., and A.L.) programs. A.L. also acknowledges a financial support from MICINN (CTQ2010-21497) of Spain.

■ REFERENCES

(1) (a) Lewis, N. S.; Nocera, D. G. *Proc. Natl. Acad. Sci. U.S.A.* **2006**, *103*, 15729. (b) Eisenberg, R.; Gray, H. B. *Inorg. Chem.* **2008**, *47*, 1697. (c) Kanan, M. W.; Nocera, D. G. *Science* **2008**, *321*, 1072. (d) Gray, H. B. *Nat. Chem.* **2009**, *1*, 7.

(2) Faunce, T. A.; Lubitz, W.; Rutherford, A. W. B.; MacFarlane, D.; Moore, G. F.; Yang, P.; Nocera, D. G.; Moore, T. A.; Gregory, D. H.; Fukuzumi, S.; Yoon, K. B.; Armstrong, F. A.; Wasielewski, M. R. *Energy Environ. Sci.* **2013**, *6*, 695.

(3) (a) Momirlan, M.; Veziroglub, T. N. *Int. J. Hydrogen Energy* **2005**, *30*, 795. (b) Dunn, S., In *Encyclopedia of Energy*, Elsevier Inc.: Amsterdam, 2004; Vol. 3, pp 241.

(4) (a) Turner, J. A. *Science* **2004**, *305*, 972. (b) Kerr, R. A.; Service, R. F. *Science* **2005**, *309*, 101.

(5) (a) Fukuzumi, S. *Eur. J. Inorg. Chem.* **2008**, 1351. (b) Fukuzumi, S.; Yamada, Y.; Suenobu, T.; Ohkubo, K.; Kotani, H. *Energy Environ. Sci.* **2011**, *4*, 2754. (c) Fukuzumi, S.; Yamada, Y. *J. Mater. Chem.* **2012**, *22*, 24284.

(6) (a) Du, P.; Eisenberg, R. *Energy Environ. Sci.* **2012**, *5*, 6012. (b) Le Goff, A.; Artero, V.; Jousselme, B.; Tran, P. D.; Guillet, N.; Metaye, R.; Fihr, A.; Palacin, S.; Fontecave, M. *Science* **2009**, *326*, 1384.

(7) Dempsey, J. L.; Brunschwig, B. S.; Winkler, J. R.; Gray, H. B. *Acc. Chem. Res.* **2009**, *42*, 1995.

(8) (a) Thoi, V. S.; Sun, Y.; Long, J. R.; Chang, C. J. *Chem. Soc. Rev.* **2013**, *42*, 2388. (b) Wang, M.; Chen, L.; Sun, L. *Energy Environ. Sci.* **2012**, *5*, 6763. (c) Lossea, S.; Vosc, J. G.; Rau, S. *Coord. Chem. Rev.* **2010**, *254*, 2492.

(9) (a) Esswein, A. J.; Nocera, D. G. *Chem. Rev.* **2007**, *107*, 4022. (b) Sun, L. C.; Akermark, B.; Ott, S. *Coord. Chem. Rev.* **2005**, *249*, 1653. (c) Wang, M.; Na, Y.; Gorlov, M.; Sun, L. *Dalton Trans* **2009**, 6458.

(10) (a) Chao, T.-H.; Espenson, J. H. *J. Am. Chem. Soc.* **1978**, *100*, 129. (b) Bakac, A.; Espenson, J. H. *J. Am. Chem. Soc.* **1984**, *106*, 5197.

(11) (a) Marinescu, S. C.; Winkler, J. R.; Gray, H. B. *Proc. Natl. Acad. Sci. U.S.A.* **2012**, *109*, 15127. (b) Stubbert, B. D.; Peters, J. C.; Gray, H. B. *J. Am. Chem. Soc.* **2011**, *133*, 18070. (c) Jacques, P.-A.; Artero, V.; Pécaut, J.; Fontecave, M. *Proc. Natl. Acad. Sci. U.S.A.* **2009**, *106*, 20627. (d) Dempsey, J. L.; Winkler, J. R.; Gray, H. B. *J. Am. Chem. Soc.* **2010**, *132*, 1060. (e) Dempsey, J. L.; Winkler, J. R.; Gray, H. B. *J. Am. Chem. Soc.* **2010**, *132*, 16774.

(12) (a) Artero, V.; Chavarot-Kerlidou, M.; Fontecave, M. *Angew. Chem., Int. Ed.* **2011**, *50*, 7238. (b) Sun, Y.; Bigi, J. P.; Piro, N. A.; Tang, M. L.; Long, J. R.; Chang, C. J. *J. Am. Chem. Soc.* **2011**, *133*, 9212. (c) Lee, C. H.; Dogutan, D. K.; McGuire, R.; Nocera, D. G. *J. Am. Chem. Soc.* **2011**, *133*, 8775. (d) Anxolabéhere-Mallart, E.; Costentin, C.; Fournier, M.; Nowak, S.; Robert, M.; Savéant, J.-M. *J. Am. Chem. Soc.* **2012**, *134*, 6104.

(13) (a) McNamara, W. R.; Han, Z.; Yin, C.-J.; Brennessel, W. W.; Holland, P. L.; Eisenberg, R. *Proc. Natl. Acad. Sci. U.S.A.* **2012**, *109*, 15594. (b) Shan, B.; Baine, T.; Ma, X. A. N.; Zhao, X.; Schmehl, R. H. *Inorg. Chem.* **2013**, *52*, 4853. (c) Mondal, B.; Sengupta, K.; Rana, A.; Mahammed, A.; Botoshansky, M.; Dey, S. G.; Gross, Z.; Dey, A. *Inorg. Chem.* **2013**, *52*, 3381. (d) Lakadamyali, F.; Kato, M.; Muresan, N. M.; Reisner, E. *Angew. Chem., Int. Ed.* **2012**, *51*, 9381.

(14) (a) Guttentag, M.; Rodenberg, A.; Bachmann, C.; Senn, A.; Hamm, P.; Alberto, R. *Dalton Trans.* **2013**, *42*, 334. (b) Utschig, L. M.; Silver, S. C.; Mulfort, K. L.; Tiede, D. M. *J. Am. Chem. Soc.* **2011**, *133*, 16334. (c) McCrory, C. C. L.; Uyeda, C.; Peters, J. C. *J. Am. Chem. Soc.* **2012**, *134*, 3164. (d) Hu, X.; Brunschwig, B. S.; Peters, J. C. *J. Am. Chem. Soc.* **2007**, *129*, 8988.

(15) (a) Solis, B. H.; Hammes-Schiffer, S. *J. Am. Chem. Soc.* **2011**, *133*, 19036. (b) McNamara, W. R.; Han, Z.; Alperin, P. J.; Brennessel, W. W.; Holland, P. L.; Eisenberg, R. *J. Am. Chem. Soc.* **2011**, *133*, 15368. (c) Sun, Y.; Sun, J.; Long, J. R.; Yang, P.; Chang, C. J. *Chem. Sci.* **2013**, *4*, 118.

(16) Szymczak, N. K.; Berben, L. A.; Peters, J. C. *Chem. Commun.* **2009**, 6729.

(17) Fukuzumi, S.; Mandal, S.; Mase, K.; Ohkubo, K.; Park, H.; Benet-Buchholz, J.; Nam, W.; Llobet, A. *J. Am. Chem. Soc.* **2012**, *134*, 9906.

(18) It should be noted that the excess $Co(Cp)_2$ reacts with CF_3COOH in MeCN at 298 K to produce $Co(Cp)_2^+$ and H_2 without $\mathbf{1}^{4+}$. Thus, $\mathbf{1}^{4+}$ was reduced by $Co(Cp)_2$, and then CF_3COOH was added to determine the H_2 yield.

(19) In presence of CF_3COOH, the $Co^{II}Co^{II}$ complex exhibited EPR spectra with low-field board absorptions centered at $g = 5.2$ along with hyperfine splitting centered at $g = 2.18$. This feature originated probably due to the coordination of trifluoroacetate anion to the Co centers, which prohibit antiferromagnetic coupling between the two Co centers.